

# Liquid phase deposition of polymers on arbitrary shaped surfaces and their suitability for e-beam patterning

B Päivänranta<sup>1</sup>, M Pudas<sup>2</sup>, O Pitkänen<sup>2</sup>, K Leinonen<sup>1</sup>,  
M Kuittinen<sup>1</sup>, P-Y Baroni<sup>3</sup>, T Scharf<sup>3</sup> and H-P Herzig<sup>3</sup>

<sup>1</sup> University of Joensuu, Department of Physics and Mathematics, PO Box 111,  
FL-80101 Joensuu, Finland

<sup>2</sup> University of Oulu Microelectronics and Material Physics Laboratories and Empart Research  
Group of Infotech Oulu, Linnanmaa, PO Box 4500, FL-90014 Oulu, Finland

<sup>3</sup> University of Neuchâtel, Institute of MicroTechnology, A.-L. Breguet 2, 2000 Neuchâtel,  
Switzerland

E-mail: [birgit.paivanranta@joensuu.fi](mailto:birgit.paivanranta@joensuu.fi)

Received 7 November 2008, in final form 18 March 2009

Published 12 May 2009

Online at [stacks.iop.org/Nano/20/225305](http://stacks.iop.org/Nano/20/225305)

## Abstract

We present a straightforward low cost liquid phase deposition method to coat arbitrary-shaped dielectric substrates with uniform electron beam sensitive polymer films. Furthermore, we investigate the use of electron beam lithography to pattern the coated pre-form substrates. The polymers studied are poly-methyl-methacrylate with different molecular weights, poly(methyl methacrylate-co-ethyl acrylate) and methyl methacrylate. The polymer coverage over the whole surface area is shown to be uniform and the thickness of the film dependent on the concentration of the polymer liquid used. As the uniform polymer layer is deposited on non-flat surfaces, we show that with an electron beam various surfaces, e.g. microlens arrays, can be re-patterned accurately with nanoscale features. Furthermore, we show the required dose for electron beam exposure to be dependent on the concentration and on the molecular weight of the polymer used.

(Some figures in this article are in colour only in the electronic version)

## 1. Introduction

Devices containing micro and nanoscale structures cover applications from industrial equipment to ordinary consumer instruments, and the number of applications is growing widely. New materials and new generation technologies have enabled the design of fabrication tools capable of smaller and smaller feature sizes. For the desired outcome one can choose the best fabrication method in terms of resolution, throughput or flexibility. However, majority of studies are focused on structuring flat substrates.

At present, the interest towards patterning non-flat substrates is growing. These interests lie e.g. in the field of micro-optics, MEMS, MOEMS and biophotonics. Many manufacturing methods, which were originally designed to pattern flat substrates, have been extended to cover the

structuring of non-planar surfaces as well, such as diamond milling [1], focused ion beam writing [2], laser lithography [3], and the use of self-organizing systems [4]. Some of these techniques, especially fast laser based systems, have been mainly used to pattern non-planar surfaces having a large radius of curvature, but they are not adequate in terms of resolution when nanoscale structures are wanted. On the other hand, focused ion beam enables the fabrication of nanoscale features and has been reported to machine substrates having as small as a 40 nm radius of curvature [5], but the patterned area is rather small.

Electron beam lithography (EBL) is a widely used method to pattern small features. In addition, as it has a fairly high sharpness of focus, it can also be extended to pattern non-planar substrates [6]. The resolution obtainable in component fabrication is not primarily limited by the optics of the EBL

machine but by the resolution of the resist materials used [7]. In recent years advances in material research have enabled resists with higher sensitivities but not necessarily higher resolutions [8]. In principle the resists used in lithographic processes should possess properties such as high resolution, adequate contrast and good adhesion to the substrate in use. However, even then, one additional challenge lies in the coating of non-flat substrates. Most conventional coating methods, spin and spray coating, have some limitations when non-planar substrates are processed, and some studies report electrodeposition to be a good alternative for this application [9, 10]. However, the latter method requires special equipment and processing and is thus not suitable for some applications.

Polymethylmethacrylate (PMMA) is traditionally classified as a high resolution positive-tone EBL resist even though it is known to suffer from scattering of electrons. Regardless of this, studies report fabrication of small feature size elements using PMMA by tuning the development process [11]. Historically, PMMA has been a widely surveyed material ever since the late 1960 when EBL started to become a more popular method to realize components with small features. This polymer is easily pre-processed by spin coating or spray coating [9] and also easily post-processed. Of the pre-processing methods the spin coating is the most widely used, as it enables coating of thin or thick films with excellent film uniformity. However, when non-flat surfaces are coated, the process becomes unsatisfactory in most cases as the centrifugal force becomes too dominant. Some numerical and experimental methods have been developed to overcome this problem, but the solutions are applicable only for some specific cases. On the other hand, spray coating enables coating of pre-form substrates as the resist is sprayed through a nozzle onto the surface. However, the layer uniformity is only good when thick films are processed.

Herein we demonstrate a simple technique to deposit PMMA of different molecular weights, methyl methacrylate (MMA) and poly(methyl methacrylate-co-ethyl acrylate) P(MMA-co-EA) co-polymer on substrates. Dielectric surfaces are coated by precipitation on the immersed sample and the method is here called the liquid phase deposition method (LPDM). This method resembles the dip coating method that has previously been used, especially in sol-gel processes, to form thin dielectric films and film stacks [12]. We show that with optimized coating parameters the deposition of the polymers on arbitrary shaped surfaces is feasible whether uniform thick or thin layers are needed. This technique enables the coating of highly concave/convex surfaces, surfaces with some height variations, and flat surfaces. Furthermore, we investigate the resist's usability in fabrication of small feature size elements by using EBL and show that both the flat and non-flat substrates can be nanopatterned with reasonable accuracy. In section 2 the resist processing is given in detail, while section 3 concentrates on electron beam exposure of the resist. Finally, results and conclusions are given in section 4.

## 2. Polymer processing

Preliminary polymer processing was performed to determine the solubility of different PMMA grades in toluene and

acetone. It was found that acetone evaporated too fast leaving a rough surface, whereas toluene was able to dissolve all the polymers tested resulting in a uniform surface. Following this, the actual polymer processing was carried out at room temperature in two steps. In the first stage the usability and behaviour of P(MMA-co-EA) was studied and in the second stage, different PMMA and MMA grades were tested. The molecular formula for the P(MMA-co-EA) was  $[\text{CH}_2\text{C}(\text{CH}_3)(\text{CO}_2\text{CH}_3)]_m[\text{CH}_2\text{CH}(\text{CO}_2\text{C}_2\text{H}_5)]_n$ , for PMMA  $[\text{CH}_2\text{C}(\text{CH}_3)(\text{CO}_2\text{CH}_3)]_n$  and for MMA  $\text{CH}_2:(\text{CH}_3)\text{COOCH}_3$  [13, 14]. The PMMA grades and P(MMA-co-EA) polymers were manufactured by Aldrich and the MMA polymer, with the trade name Degalan LP 50-02, was manufactured by Röhm GmH & Co. KG. During the experimental tests all the polymers were dissolved in toluene (Aldrich 99.8%). The P(MMA-co-EA) having a molecular weight ( $M_w$ ) of 90k is referred to here as sample **a**, the different PMMA grades,  $M_w = 15\text{k}$ ,  $M_w = 120\text{k}$  and  $M_w = 996\text{k}$ , are referred to as samples **b–d**, respectively, and the MMA polymer with a molecular weight of  $M_w = 60\text{k}$  is referred to as sample **e**.

The solubility for each polymer was tested by dissolving the maximum amount of solid polymer in toluene. An excess amount of polymer was mixed in toluene, and afterwards the dissolved solution was extracted. With this process, and with 24 h mixing time, the abundant concentration of 12% was achieved for the sample **a**. The polymer materials **b–e** were tested by dissolving the samples in 10–20% concentration. It was found that even after dissolving over long time (over three days) some polymer remained still solid. It was also found that, with concentrations over 10%, defects (surface waviness) started to appear in the surface coating. The solubility values obtained for all the samples are shown in table 1.

The coating properties were studied by placing the solvent and the polymer in a beaker with a magnetic mixer and with a sample holder. Before inserting the sample, the solution was mixed for 5 min, so that the maximum concentration of polymer in liquid was exceeded. After mixing, the sample **a** was placed in the liquid in a horizontal plane. After the coating step the sample was hardened and annealed by baking it in oven for 5–10 min at 80–100 °C. In order to verify the thickness of the obtained P(MMA-co-EA) layer, part of the layer was peeled off with adhesive tape, however, in most cases, the peeling had to be done by scraping with a knife blade. The coating thickness obtained was measured with Dektak ST surface profiler, and it was found that within measurable limits, the thickness  $h$  in nanometres changed linearly with respect to time according to  $h = \sim 3t$ , where  $t$  is time in seconds.

In order to verify the effect of evaporation time on the solvent and the critical concentration limit, sample **d** was coated for 10 s at different times from the commencement of mixing. Figure 1 shows the average thicknesses and deviations of thickness for the sample **d** having an abundant concentration of >10%. It can be seen that both the thickness values decrease as a function of the time from the commencement of the mixing. This indicates that, before the solvent is evaporated, the highly concentrated solution has unstable coating properties and for this reason is not suitable for this case. Also, by changing the coating time from 10 to 100 s

**Table 1.** Summary of the properties of the tested polymers with different molecular weights ( $M_w$ ). The solubility gives the maximum concentration that can be obtained with each polymer and the used concentration shows the concentration of the solution that is used in the exposure tests.

Label	Sample a	Sample b	Sample c	Sample d	Sample e
Manufacturer	Aldrich	Aldrich	Aldrich	Aldrich	Röhm
CAS	9010-88-2	9011-14-7	9011-14-7	9011-14-7	80-62-6
Type	P(MMA-co-EA)	PMMA	PMMA	PMMA	MMA
$M_w$ (k)	90	15	120	996	60
Solubility (%)	12	9	9	>10	>20
Used concentration (%)	2	1.3	1.2	1.3/1.8	1.8
Coating thickness (nm) <sup>a</sup>	300 <sup>b</sup>	78	120	113/176	101

<sup>a</sup> Samples were coated for 100 s.

<sup>b</sup> Sample coating follows an estimation  $h = \sim 3t$ .

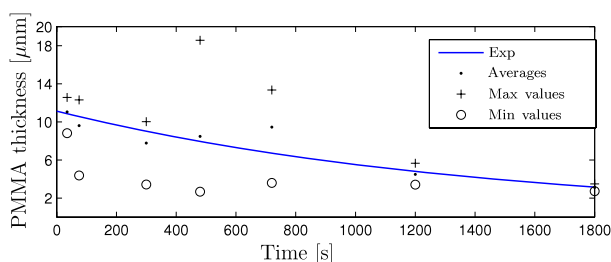


**Figure 1.** Effect of starting time on PMMA ( $M_w = 996k$ , concentration 10%) coating thickness, with a 10 s coating time. It can be seen that the average thicknesses, as well as the deviation of the thicknesses, decrease as a function of time.

for the sample e, the thickness variation of the polymer remains small at all the concentrations studied. For the MMA polymer see figure 2. By fitting an exponential curve to the measurement points, the film thickness  $h$  in nanometres for 10 s coating time can be shown to follow the exponentially growing curve  $h = -615.55 + 592.24e^{0.11c}$ , where  $c$  is the concentration of the liquid. For this curve, the  $R^2$ -value, the coefficient of determination, is calculated to be 0.9998. For 100 s coating time the function of thickness follows a quite similar curve,  $h = -512.56 + 497.77e^{0.118c}$ . For this function the  $R^2$ -value is 0.9999. The average polymer coating thicknesses obtained with 100 s coating time for all the grades are shown in table 1.

In conclusion, it was found that the obtained thickness was dependent on the concentrations used and that the higher concentrations give thicker polymer films. As the polymer grades were also to be tested in nanostructure fabrication, for which thin layers, 100–200 nm, are required, low concentration solutions (1–2%) were made for all the polymer grades. The concentrations used are shown in table 1.

### 3. Sample preparation and experimental results

For the exposures we used a Vistec EBP 5000 + ES HR, which is a Gaussian shaped electron beam patterning tool with a maximum acceleration voltage of 100 kV. Conventionally, as electron beam lithography is only used with planar substrates, the resolution is good at the point where the electron beam is focused onto the substrate by using the final lens in the

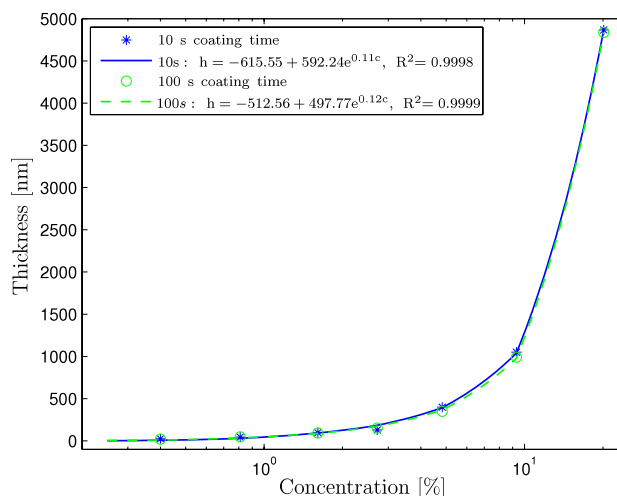


**Figure 2.** The concentration dependences on the total thickness for two coating times, 10 and 100 s, for the MMA ( $M_w = 60k$ ) polymer are shown to be alike. Also, for both the coating times a well conforming exponential fit can be found to estimate the correlation between the thickness and the concentration.

optical column. However, if the sample has some pre-form, the system installed in-house is incapable of measuring the height correctly because the optical measurement system is based on the specular reflectance. As the height is measured from a non-flat surface, the laser beam no longer reaches the detector and *in situ* measurement during the patterning cycle is not possible. For this reason the height measurement has to be turned off and the correct height for the exposure has to be determined manually before the exposure. Furthermore, as the pre-form substrates are exposed with a single height value, the maximum focus depth of the electron beam has to be reached in order to result in accurate patterning. This can be done by setting the final aperture, which is stationed inside the optical column just before the final lens which focuses the electron beam on the substrate, to the smallest possible value (in our case 200  $\mu\text{m}$ ) and selecting the main field (the area which is patterned without moving the substrate) in the pattern to be as small as possible to minimize the pattern distortion.

#### 3.1. Patterning flat substrates

To determine the exposure dose needed to pattern the polymers studied, flat substrates were coated with polymers by using



**Table 2.** Optimal exposure doses needed to result in 250 nm L/S for the polymers studied by using 220 nm exposure lines.

Polymer ( $M_w$ )	Concentration (%)	Exposure dose ( $\mu\text{C cm}^{-2}$ )
PMMA 15k	1.3	120
PMMA 120k	1.2	200
PMMA 996k	1.3	250
PMMA 996k	1.8	400
MMA 60k	1.8	350
P(MMA-co-EA) 90k	2	275

LPDM. To avoid charging of the samples during the exposure a 30 nm copper layer was evaporated on top of the resist of all exposed samples as a conductive layer. All the samples were exposed with a variety of doses, in order to find the correct dose value for each of the polymers, by using 220 nm exposure lines in resulting in a 250 nm line-to-space ratio (L/S) grating. After exposure, all samples were developed in a solution of methyl iso-butyl ketone and isopropanol. The linewidths obtained were measured with a scanning electron microscope (SEM). As expected, it was found that the optimal dose value is dependent on the concentration and on the molecular weight of the polymer. For example, the PMMA with an  $M_w$  of 15k is overdosed when the dose is  $250 \mu\text{C cm}^{-2}$  whereas this amount is optimal for PMMA with an  $M_w$  of 996k and a concentration of 1.3%. However, for PMMA ( $M_w$  of 996k) with a higher concentration of 1.8% the adequate dose was found to be larger,  $400 \mu\text{C cm}^{-2}$ . Differences were also found between the different polymer types as the MMA with a lower  $M_w$  of 60k and a concentration of 1.8% has close to the same optimal dose as the PMMA with  $M_w$  of 996k having the same concentration. In table 2 the optimal exposure doses for all the polymers with a fixed grating pattern are shown. In figure 3 the effect of the dose on the linewidth is illustrated in more detail. It can clearly be seen that the linewidth quality with different materials and different doses behaves alike. It must, however, be noted that, in these exposure tests, the proximity effect was not considered.

The focus offset tests were done in order to determine the effect of a non-focused beam diameter on the desired linewidth. The test was carried out by using standard flat silicon dioxide substrates having a 150 nm P(MMA-co-EA) layer deposited by using LPDM. The height was measured from the flat surface and the focus was offset manually from 0 to  $\pm 20 \mu\text{m}$ . After development the linewidths were measured with the SEM. The offset effect on the grating linewidth over a  $40 \mu\text{m}$  focus range was observed to be 50 nm. The line broadening  $\Delta d$  caused by the height offset change can also be estimated numerically by using simple geometry,

$$\Delta d = \frac{(a) * h_{\text{off}}}{\text{WD}}, \quad (1)$$

where  $a$  is the final aperture of the e-beam,  $h_{\text{off}}$  the focus offset, and WD the working distance. By substituting the aperture size  $a = 200 \mu\text{m}$ , maximum height offset  $h_{\text{off}} = \pm 20 \mu\text{m}$ , and working distance  $\text{WD} = 40 \text{ mm}$  in equation (1), we get the upper limit for the line broadening,  $\Delta d = 100 \text{ nm}$ . However,

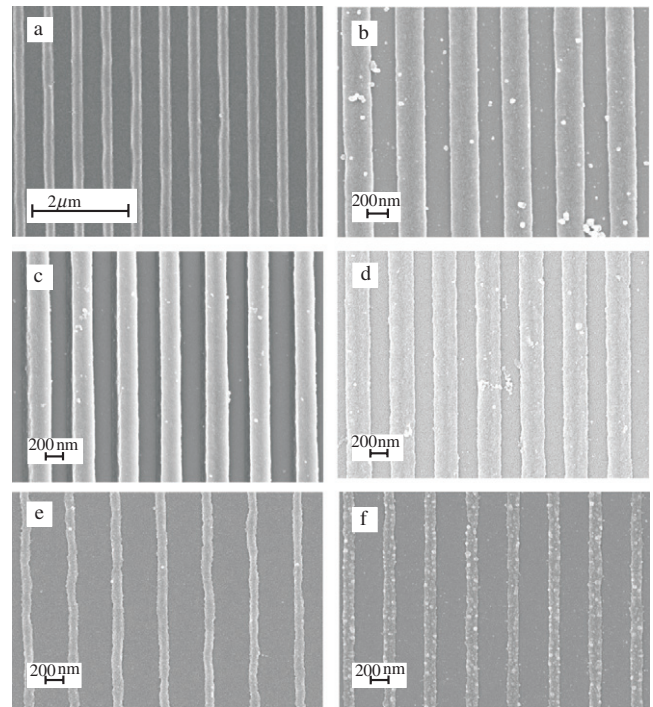


**Figure 3.** Polymers exposed with different doses, (a) P(MMA-co-EA) with  $300 \mu\text{C cm}^{-2}$ , (b) MMA with  $400 \mu\text{C cm}^{-2}$ , (c) PMMA (996k and 1.8%) with  $350 \mu\text{C cm}^{-2}$ , (d) PMMA (996k and 1.3%) with  $250 \mu\text{C cm}^{-2}$ , (e) PMMA (120k) with  $650 \mu\text{C cm}^{-2}$ , and (f) PMMA (15k) with  $250 \mu\text{C cm}^{-2}$ . These results indicate that all the polymers are well-suited for electron beam patterning and that the molecular weight, as well as the concentration of the polymer, affect the exposure dose.

as we also need to take into account the spot size  $d_0 = 40 \text{ nm}$  of the beam, the actual linewidth broadening is  $60 \text{ nm}$  for a  $40 \mu\text{m}$  focus variation. This is close to the value that we obtained from experimental measurements, see figure 4. It must be noted here that these results were obtained by using the optimal dose needed for the patterning. When a greater dose value is used the linewidth spreading accelerates and these results are no longer valid.

### 3.2. Patterning pre-form substrates

For the exposure of non-flat substrates we used two kinds of pre-form samples. The first set of pre-form substrates were silica samples having a binary structure (pixel size  $5 \mu\text{m}$ , height  $700 \text{ nm}$ ) fabricated by EBL, and the second set of samples consisted of arrays of spherical microlenses. The microlenses were fabricated into silica with a standard reflow process, in which resist pillars form spherical shapes due to external heating [15]. The microlenses studied had a diameter of  $145 \mu\text{m}$  and a height of  $18 \mu\text{m}$ .

Firstly, the P(MMA-co-EA) coated microlens array was used to check the resist layer uniformity obtained. The thickness was examined from the cross section of the coated sample by using the SEM. It was seen that the layer thickness stayed constant regardless of the shape of the surface, see figure 5. The average layer thickness after 30 s coating was  $75 \text{ nm}$  and the total thickness variation over the lens

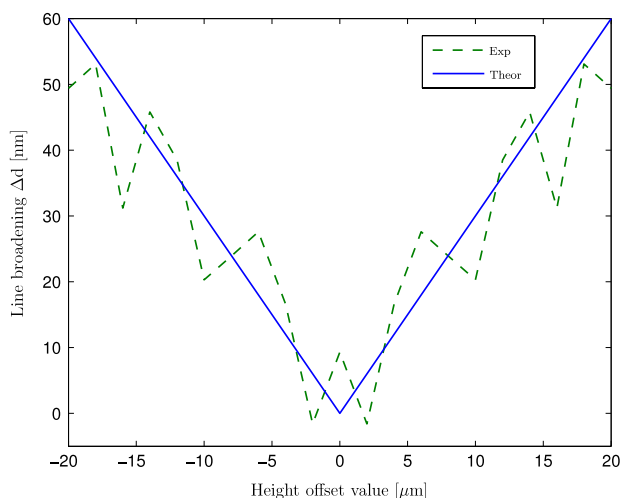


**Figure 4.** The experimental (---) and estimated theoretical (—) focus offset dependence on the grating linewidth. Over the  $\pm 40 \mu\text{m}$  offset range the exposed linewidth spreads 50 nm experimentally.

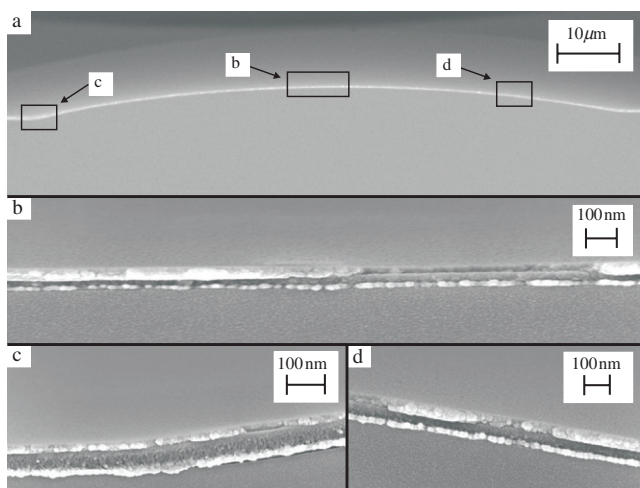


**Figure 5.** The resist thickness at different points of the microlens (a). Resist thickness on the top of microlens (b), in the ‘corner’ between the microlens and flat (c), on the bottom flat area (d). The variation of thicknesses over these areas is 6%.

surface was 6%. For the following exposure tests the pre-form substrates were coated with P(MMA-co-EA) for 50 s resulting in a film thickness of 150 nm.

Secondly, the pre-form shaped samples were patterned with a nanostructure consisting of  $180 \text{ nm} \times 180 \text{ nm}$  pillars in a  $250 \text{ nm}$  grid. The pre-form substrate with a micron-scale binary structure patterned with a nanostructure is shown in figure 6. Because the height difference between the two areas is small (700 nm) the linewidth in both of the areas remains practically the same. For the microlens samples, the height was mapped from a flat reference area outside of the microlens array area prior to the exposure. Half of the height of the microlens array was added to this measured reference height. In the outermost areas, where the focus offset is  $9 \mu\text{m}$ , i.e., between the microlenses and in the vertex of the microlenses, the nanostructure is patterned identically. The nanostructure

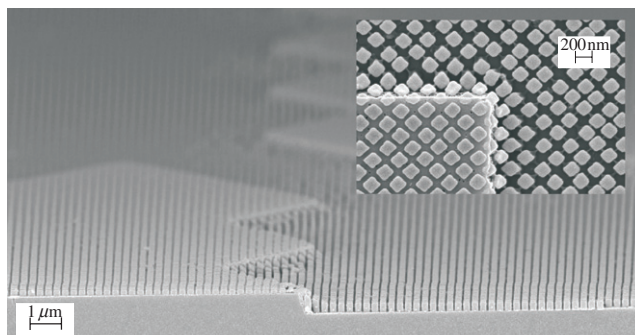


**Figure 6.** Substrate having a micron-scale structure. The substrate is coated with P(MMA-co-EA) and exposed with an electron beam. An enlargement of the structure is shown in the inset, where the lower left corner is 700 nm higher than the surrounding area.

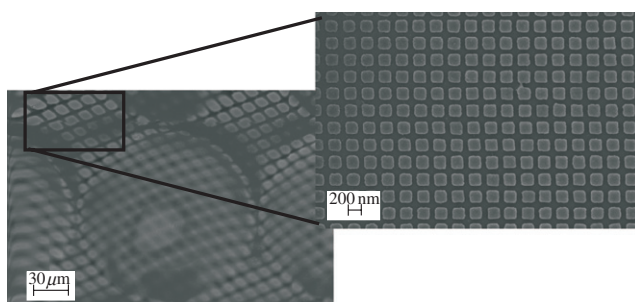


**Figure 7.** Microlenses patterned with a nanoscale structure. The area between the microlenses is magnified. (Structure features in the left hand figure are not seen in the real scale because of aliasing caused by digital image sampling [16].)

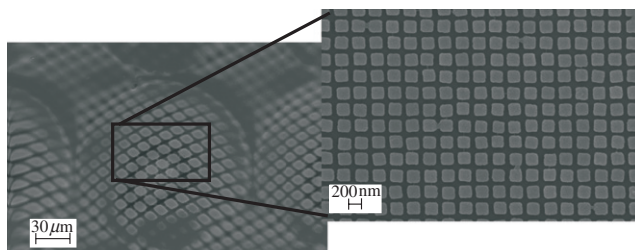


**Figure 8.** Microlenses patterned with a nanoscale structure. The area on the top of the microlenses is magnified. (Structure features in the left hand figure are not seen in the real scale because of aliasing caused by digital image sampling [16].)

in the bottom and top regions of the microlens array can be seen the figures 7 and 8, respectively. As the height of the microlens shown is  $18 \mu\text{m}$  the theoretical overall variation of the nanopattern linewidth over the single microlens is  $\sim 22 \text{ nm}$ . However, the measured linewidth spreading over the microlens was measured to be slightly smaller,  $\sim 17 \text{ nm}$ . The reason for the smaller experimental value obtained can be found from the dose used, as here an optimal dose needed for the patterning was used.

#### 4. Conclusions

We have demonstrated a simple method to coat dielectric silica substrates with different types of electron beam sensitive polymers and furthermore we checked the suitability of these polymer materials in electron beam lithography. We studied three different polymer materials, P(MMA-co-EA), PMMA and MMA with different concentrations and molecular weights. By choosing the polymer with optimal molecular weight and by optimizing the coating time and liquid concentration, uniform film thicknesses are obtained on both flat and arbitrary shaped surfaces. For sample **a** the coating thickness was shown to change as a function of time, and for the samples **b–e** instead of time, the coating thickness was dependent on the concentration. Also, it was observed that the thin films formed with higher molecular weights were more durable than films with lower molecular weights.

From the exposure tests performed it can be concluded that the higher the concentration and the molecular weight, the higher the dose needed for the polymer exposure. In electron beam exposure tests we used flat substrates and pre-patterned substrates having a micron-scale structure and microlens arrays. After coating the pre-form substrates with LPDM, they were re-patterned with a nanostructure by using a high-voltage electron beam. For the majority of the exposure tests we used P(MMA-co-EA) with a molecular weight of 90k and coated the samples for 50 s in a P(MMA-co-EA) solution having a ~2% concentration in order to obtain a 150 nm layer thickness. When non-flat surfaces were patterned, the measured change in the linewidth over the  $\pm 20 \mu\text{m}$  focus offset range was 50 nm, and during the exposure tests the resolution of the nanostructure remained good. For fabrication of micron-scale structures the focus offset error is fractional and with nanoscale structures the error has to be taken into account with respect to the application in mind.

Further work could address the material and process development, to fine tune the sharp edge coverage, especially in such applications where improved coating properties are needed. This should be possible, with e.g. repeated coating-drying cycles and material modifications.

#### Acknowledgments

The corresponding author wishes to acknowledge the funding given by the 'Finnish Funding Agency for Technology and Innovation' (TEKES). This work was also funded in part by the European Regional Development Fund (ERDF) project, 'Nanoresolution tools for interdisciplinary application', funded by the Provincial State Office of Oulu. In addition, funding from 'The Research and Development Project on Nanophotonics', funded by the Finnish Ministry of Education is acknowledged. Furthermore, the authors want to express their gratitude to the European Joint Research Network 'Network of Excellence on Micro-Optics' (NEMO).

#### References

- [1] Karlsson M and Nikolajeff F 2003 *Opt. Express* **11** 502–7
- [2] Tseng A A 2004 *J. Magn. Magn. Mater.* **14** R15–34
- [3] Radtke D and Zeitner U D 2007 *Opt. Express* **15** 1167–74
- [4] Park M, Chaikin P M, Register R A and Adamson D H 2001 *Appl. Phys. Lett.* **79** 257–9
- [5] Picard Y N, Adams D P, Vasile M J and Ritchey M B 2003 *Proc. Eng.* **27** 59–69
- [6] Kley E B, Thoma F, Zeitner U D, Wittig L and Aagedal H 1998 *SPIE Proc.* **3276** 254–62
- [7] Broers A N, Hoole A C F and Ryan J M 1996 *Microelectron. Eng.* **32** 131–42
- [8] Yang H, Jin A, Luo Q, Gu C and Cui Z 2007 *Microelectron. Eng.* **84** 1109–12
- [9] Pham N P, Boellard E, Sarro P M and Burghartz J N 2002 *Proc. 5th Semiconductor Advances for Future Electronics Workshop* pp 81–6
- [10] Babin S and Koops H W P 1996 *J. Vac. Sci. Technol. B* **14** 3860–3
- [11] Hu W W, Sarveswaran K, Lieberman M and Bernstein G H 2004 *J. Vac. Sci. Technol. B* **22** 1711–6
- [12] Klein L C 1988 *Sol–Gel Technology for Thin Films, Fibers, Preforms, Electronics, and Specialty Shapes* (New Jersey: Noyes Publications)
- [13] URL= <http://www.sigmaaldrich.com>
- [14] URL= <http://www.roehm.de>
- [15] Daly D 1990 *Meas. Sci. Technol.* **1** 759–66
- [16] Lathi B P 1998 *Modern Digital and Analog Communication Systems* (Oxford: Oxford University Press)